Research Article

Chaudry Masood Khalique* and Mduduzi Yolane Thabo Lephoko

Novel constructed dynamical analytical solutions and conserved quantities of the new (2+1)-dimensional KdV model describing acoustic wave propagation

https://doi.org/10.1515/phys-2025-0124
received June 08, 2024; accepted November 25, 2024

Abstract: In this study, we delve into the exploration of the new (2+1)-dimensional KdV model, a mathematical model essential to the understanding of various nonlinear phenomena such as ion acoustic waves and harmonic crystals. The primary objective of this study is to conduct a comprehensive symmetry analysis of the model, a method that has not been previously applied to the model. This approach aims to uncover new exact solutions, which will not only enrich the existing literature but also provide valuable insights for researchers specializing in symmetry analysis and the broader scientific community. To achieve this goal, we employ a comprehensive analytical methodology that combines Lie symmetry analysis technique with Kudryashov's method, the simplest equation technique, direct integration, Jacobi elliptic expansion technique, and the power series method. Through the utilization of these diverse analytical approaches, we successfully derive solutions for the model in various functional forms, including exponential, trigonometric, hyperbolic, Jacobi elliptic, and rational functions. These solutions exhibit broad applicability across diverse disciplines within nonlinear science and engineering. To provide a deeper understanding of the obtained solutions, we present our findings through visual representations, utilizing three-dimensional, two-dimensional, and density plots. By selecting appropriate ranges for the involved arbitrary constants, we effectively illustrate the dynamical wave behaviours inherent in the solutions. Notably, our visual representations reveal discernible patterns characterized by periodic and kink-shaped structures, shedding light on the intricate dynamics encapsulated within the solutions. Furthermore, we endeavour to identify conserved vectors associated with the model under investigation. To achieve this, we employ the multiplier method and Ibragimov's theorem. The results are expected to enhance our understanding of the model's physical implications and contribute to advancing the field.

Keywords: (2+1)-dimensional KdV model, Lie group analysis, exact solution, conserved vectors, multiplier method, Ibragimov's theorem

1 Introduction

The pursuit of exact solutions for nonlinear partial differential equations (NLPDEs) has gained increasing prominence. This trend is driven, in part, by the capacity of NLPDEs to effectively model real-world phenomena, finding applications across diverse scientific domains such as fluid dynamics, biology, plasma physics, fiber optics, engineering, and solitary wave theory. The literature has witnessed a substantial exploration of various mathematical and physical NLPDEs, and contemporary researchers are actively extending these investigations [1–17]. However, the challenge of obtaining exact solutions for NLPDEs persists, and the generalizability of the methods employed for one set of nonlinear equations to others is often limited. Consequently, researchers have proposed several methodologies to address these complexities. Noteworthy among these techniques are the tanh-sech method [18], Bäcklund transformation approach [19], the $\exp(-\Psi(\tau))$-expansion technique [20], Cole–Hopf transformation method [21], Painlevé expansion approach [22], the extended simplest equation method [23], and Lie symmetry technique [24,25]. These diverse methodologies provide

* **Corresponding author: Chaudry Masood Khalique,** Department of Mathematical and Statistical Sciences, Material Science Innovation and Modelling Focus Area, North-West University, Mafikeng Campus, Private Bag X2046, Mmabatho 2735, Republic of South Africa; Department of Mathematics and Informatics, Azerbaijan University, Jeyhun Hajibeyli str., 71, AZ1007, Baku, Azerbaijan, e-mail: Masood.Khalique@nwu.ac.za
Mduduzi Yolane Thabo Lephoko: Department of Mathematical and Statistical Sciences, Material Science Innovation and Modelling Focus Area, North-West University, Mafikeng Campus, Private Bag X2046, Mmabatho 2735, Republic of South Africa, e-mail: dasmice@gmail.com

valuable tools for researchers seeking to uncover exact solutions for NLPDEs and contribute to the advancement of our understanding of complex nonlinear phenomena in various scientific disciplines.

Conservation laws play a pivotal role in diverse applications, particularly in the examination of differential equations (DEs). They serve as essential tools for describing physically conserved quantities, including momentum, mass, energy, charge, and constants of motion [26]. Furthermore, conservation laws find utility in various aspects of DE investigations, encompassing the identification of integrability, linearization, determination of solution existence and uniqueness, and validation of numerical methods [27–29]. The academic literature has witnessed the proposition of multiple methodologies for identifying conservation laws. Among these, the standard multiplier method [25], Noether's approach [30], and Ibragimov's theorem [31] stand out as prominent techniques. These methodologies contribute significantly to the systematic identification and analysis of conservation laws, thereby enhancing our understanding of the underlying principles governing DEs and their applications in various scientific contexts.

The newly formulated (2+1)-dimensional KdV (2DKdV) equation serves as a mathematical model for describing nonlinear and dispersive waves, particularly those encountered in phenomena such as shallow water waves. This equation plays a significant role in elucidating various nonlinear manifestations of acoustic waves in harmonic crystals and ion-acoustic waves in plasma [32]. The 2DKdV equation is expressed as

$$u_t + \alpha u_x u_y + u_{xxy} = 0, \tag{1.1}$$

where the variable $u = u(t, x, y)$ represents the surface profile under consideration, while α denotes the nonlinear convection coefficient term. The terms in the equation have distinct physical interpretations: u_t characterizes the temporal evolution of wave propagation, $u_x u_y$ signifies the steepening of the wave, and u_{xxy} represents the spreading of the wave [32].

Several researchers have explored the proposed 2DKdV model, each contributing valuable insights to its analysis. Arif *et al.* [32] successfully derived multi-soliton solutions for the 2DKdV equation. The collisions of these solutions were analyzed through the implementation of Hirota's scheme. Yokus and Isah [33] employed the new homoclinic method based on the Hirota bilinear form to establish the bilinear form of the 2DKdV equation. Their work resulted in the discovery of numerous new exact solutions. Additionally, the stability of these solutions was rigorously examined using modulation instability as a criterion. Isah and Yokus [34] employed Hirota bilinearization methodology to derive various types of soliton solutions, notably including kink and rogue wave solutions. Raheel *et al.* [35] contributed to the understanding of the 2DKdV equation by obtaining various analytical wave solitons. Their approach involved the use of different techniques, including Hirota bilinear, $\exp_a$ function, extended sinh-Gordon equation expansion, and modified simplest equation techniques. The solutions obtained encompassed periodic waves, periodic-cross-kink waves, three-wave patterns, and other analytical wave solitons. Overall, these studies have significantly enriched the understanding of the dynamics and behaviour of the 2DKdV equation, providing a foundation for further exploration and applications. Moreover, this highlights an existing gap in the literature, *i.e.*, the model has yet to be studied through the lens of symmetry analysis.

This study aims to conduct a comprehensive symmetry analysis of the model to deepen our understanding of its dynamics. Our primary objective is to generate a diverse array of new exact and semi-analytical solutions for the 2DKdV model, utilizing a combination of analytical techniques not previously employed in its investigation. Specifically, we intend to utilize Lie group analysis, Kudryashov's method, the simplest equation approach, the Jacobi elliptic expansion technique, and the power series method to achieve this goal. Moreover, our objective is to ascertain the conservation laws inherent in the model through the utilization of the multiplier approach and conservation theorem by Ibragimov. To effectively illustrate the dynamic behaviour of solitary wave profiles associated with the newly obtained semi-analytical and soliton solutions, numerical simulations will be conducted. These simulations will incorporate various visualization methods, including three-dimensional, two-dimensional, and density plots. It is pertinent to highlight that the findings of this investigation are anticipated to be novel and, as far as we are aware, have not been documented in the current literature. Thus, this study contributes significantly to the advancement of our understanding of the 2DKdV model and its applications in nonlinear wave phenomena.

2 Lie group analysis

2.1 Symmetries of (1.1)

Let

$$\begin{aligned}
\tilde{t} &\longrightarrow t + \Re\, \tau(t, x, y, u) + O(\Re^2),\\
\tilde{x} &\longrightarrow x + \Re\, \xi(t, x, y, u) + O(\Re^2),\\
\tilde{y} &\longrightarrow y + \Re\, \Phi(t, x, y, u) + O(\Re^2),\\
\tilde{u} &\longrightarrow u + \Re\, \eta(t, x, u) + O(\Re^2),
\end{aligned}$$

be the one-parameter Lie group of infinitesimal transformations of the 2DKdV model (1.1), whereby the group

parameter $\Re$ and τ, ξ, Φ, and η are used to obtain Lie point symmetries of the underlying model. The requirement is that Eq. (1.1) will admit the vector field C defined by

$$C = \tau\frac{\partial}{\partial t} + \xi\frac{\partial}{\partial x} + \Phi\frac{\partial}{\partial y} + \eta\frac{\partial}{\partial u},$$

provided that the invariance condition

$$C^{[3]}(u_t + \alpha u_x u_y + u_{xxy} = 0)|_{1.1} = 0 \tag{2.1}$$

holds, whenever $u_t + \alpha u_x u_y + u_{xxy} = 0$. Specifically, $C^{[3]}$ connotes the third-order prolongation of C, in this case written as [25]

$$C^{[3]} = C + \zeta_t\frac{\partial}{\partial u_t} + \zeta_x\frac{\partial}{\partial u_x} + \zeta_y\frac{\partial}{\partial u_y} + \zeta_{xxy}\frac{\partial}{\partial u_{xxy}}.$$

It is observed that expanding and splitting Eq. (2.1) over derivatives of u eventually guarantee the system:

$$\begin{aligned}
&\Phi_x = 0, \tau_x = 0, \eta_{yu} = 0, \xi_y = 0, \tau_y = 0, \eta_{uu} = 0, \Phi_u = 0,\\
&\xi_u = 0, \tau_u = 0,\\
&\eta_t + \eta_{xxy} = 0, \eta_u + \xi_x = 0, \xi_t - \alpha\eta_y = 0, 2\eta_{xu} - \xi_{xx} = 0,\\
&\Phi_y - \tau_t + 2\xi_x = 0, 2\alpha\eta_x - 2\Phi_t + \xi_{xxx} = 0.
\end{aligned}$$

Solving the aforementioned system leads to the infinitesimals

$$\begin{aligned}
&\tau = \mathbf{c}_2 + \mathbf{c}_3 t, \xi = \mathbf{c}_4 + \mathbf{c}_5 t - \mathbf{c}_1 x, \Phi = \mathbf{c}_6 + \alpha\mathbf{c}_8 t + (2\mathbf{c}_1 + \mathbf{c}_3)y,\\
&\eta = \mathbf{c}_7 + \mathbf{c}_1 u + \mathbf{c}_8 x + \mathbf{c}_5\frac{y}{\alpha},
\end{aligned}$$

which yield the symmetries:

$$\begin{aligned}
&C_1 = \frac{\partial}{\partial t}, \quad C_2 = \frac{\partial}{\partial x}, \quad C_3 = \frac{\partial}{\partial y}, \quad C_4 = \frac{\partial}{\partial u},\\
&C_5 = t\frac{\partial}{\partial t} + y\frac{\partial}{\partial y}, \quad C_6 = \alpha t\frac{\partial}{\partial t} + x\frac{\partial}{\partial u}\\
&C_7 = \alpha t\frac{\partial}{\partial t} + y\frac{\partial}{\partial u}, \quad C_8 = x\frac{\partial}{\partial x} - 2y\frac{\partial}{\partial y} - u\frac{\partial}{\partial u}.
\end{aligned}$$

For the obtained symmetries, we present the commutator table and adjoint representation [25,36] (Tables 1 and 2).

Table 1: Commutator table

$[C_i, C_j]$	C_1	C_2	C_3	C_4	C_5	C_6	C_7	C_8
C_1	0	0	0	0	C_1	αC_3	αC_2	0
C_2	0	0	0	0	0	C_4	0	C_2
C_3	0	0	0	0	C_3	0	C_4	$-2C_3$
C_4	0	0	0	0	0	0	0	$-C_4$
C_5	$-C_1$	0	$-C_3$	0	0	0	C_7	0
C_6	$-\alpha C_3$	$-C_4$	0	0	0	0	0	$-2C_6$
C_7	$-\alpha C_2$	0	$-C_4$	0	$-C_7$	0	0	C_7
C_8	0	$-C_2$	$2C_3$	C_4	0	$2C_6$	$-C_7$	0

Solving the initail value problem [24,25]

$$\begin{aligned}
&\frac{d\tilde{t}}{d\Re} = \tau(\tilde{t}, \tilde{x}, \tilde{y}, \tilde{u}), \quad \frac{d\tilde{x}}{d\Re} = \xi(\tilde{t}, \tilde{x}, \tilde{y}, \tilde{u}),\\
&\frac{d\tilde{y}}{d\Re} = \Phi(\tilde{t}, \tilde{x}, \tilde{y}, \tilde{u}), \quad \frac{d\tilde{u}}{d\Re} = \eta(\tilde{t}, \tilde{x}, \tilde{y}, \tilde{u}),
\end{aligned}$$

where $\tilde{t} = t$, $\tilde{x} = x$, $\tilde{y} = y$, and $\tilde{u} = u$ at $\Re = 0$, one obtains the one-parameter groups of transformations $\mathfrak{G}_{\Re_i}(t, x, y)$, $(i = 1, 2, \ldots, 8)$, generated by C_i $(i = 1, 2, \ldots, 8)$, respectively:

$$\begin{aligned}
&\mathfrak{G}_{\Re_1} : (\tilde{t}, \tilde{x}, \tilde{y}, \tilde{u}) \longrightarrow (t + \Re, x, y, u),\\
&\mathfrak{G}_{\Re_2} : (\tilde{t}, \tilde{x}, \tilde{y}, \tilde{u}) \longrightarrow (t, x + \Re, y, u),\\
&\mathfrak{G}_{\Re_3} : (\tilde{t}, \tilde{x}, \tilde{y}, \tilde{u}) \longrightarrow (t, x, y + \Re, u),\\
&\mathfrak{G}_{\Re_4} : (\tilde{t}, \tilde{x}, \tilde{y}, \tilde{u}) \longrightarrow (t, x, y, u + \Re),\\
&\mathfrak{G}_{\Re_5} : (\tilde{t}, \tilde{x}, \tilde{y}, \tilde{u}) \longrightarrow (e^{\Re}t, x, e^{\Re}y, u),\\
&\mathfrak{G}_{\Re_6} : (\tilde{t}, \tilde{x}, \tilde{y}, \tilde{u}) \longrightarrow (t, x, y + \alpha\Re t, u + \Re x),\\
&\mathfrak{G}_{\Re_7} : (\tilde{t}, \tilde{x}, \tilde{y}, \tilde{u}) \longrightarrow (t, x + \alpha\Re t, y, u + \Re y),\\
&\mathfrak{G}_{\Re_8} : (\tilde{t}, \tilde{x}, \tilde{y}, \tilde{u}) \longrightarrow (t, e^{\Re}x, e^{-2\Re}y, e^{-\Re}u).
\end{aligned}$$

Theorem 2.1. *Given the 2DKdV model, since each group $\mathfrak{G}_{\Re_i}$ is a symmetry group, if $u(t, x, y) = \mathfrak{S}(t, x, y)$ satisfies the model, then the functions*

$$\begin{aligned}
&u_1 = \mathfrak{S}(t - \Re, x, y), \quad u_2 = \mathfrak{S}(t, x - \Re, y),\\
&u_3 = \mathfrak{S}(t, x, y - \Re), \quad u_4 = \mathfrak{S}(t, x, y) + \Re,\\
&u_5 = \mathfrak{S}(e^{-\Re}t, x, e^{-\Re}y), \quad u_6 = \mathfrak{S}(t, x, y - \alpha\Re t) + \Re x,\\
&u_7 = \mathfrak{S}(t, x - \alpha\Re t, y) + \Re y, \quad u_8 = e^{-\Re}\mathfrak{S}(t, e^{-\Re}x, e^{2\Re}y)
\end{aligned}$$

also satisfy the model.

2.2 Lie symmetry reductions and solutions

This section implores the eight Lie point symmetries acquired through our analysis to undertake symmetry reductions with the objective of deriving group invariant solutions of the 2DKdV model (1.1).

Reduction 1. To derive travelling wave solutions, we contemplate the linear combination of the first three symmetries $C_1 = \partial/\partial t$, $C_2 = \partial/\partial x$, and $C_3 = \partial/\partial y$. This leads to the group invariant solution

$$u = \psi(z), z = x + by + ct.$$

Substituting the aforementioned value of u into (1.1), we secure the third-order nonlinear ordinary differential equation (NLODE)

$$b\psi'''(z) + \alpha b\psi'^2(z) + c\psi'(z) = 0. \tag{2.2}$$

Table 2: Adjoint representation

Ad	C_1	C_2	C_3	C_4	C_5	C_6	C_7	C_8
C_1	C_1	C_2	C_3	C_4	$C_5 - \varepsilon C_1$	$C_6 - \alpha\varepsilon C_3$	$C_7 - \alpha\varepsilon C_2$	C_8
C_2	C_1	C_2	C_3	C_4	C_5	$C_6 - \varepsilon C_4$	C_7	$C_8 - \varepsilon C_2$
C_3	C_1	C_2	C_3	C_4	$C_5 - \varepsilon C_3$	C_6	$C_7 - \varepsilon C_4$	$2\varepsilon C_3 + C_8$
C_4	C_1	C_2	C_3	C_4	C_5	C_6	C_7	$\varepsilon C_4 + C_8$
C_5	$e^{\varepsilon}C_1$	C_2	$e^{\varepsilon}C_3$	C_4	C_5	C_6	$e^{-\varepsilon}C_7$	C_8
C_6	$\alpha\varepsilon C_3 + C_1$	$\varepsilon C_4 + C_2$	C_3	C_4	C_5	C_6	C_7	$2\varepsilon C_6 + C_8$
C_7	$\alpha\varepsilon C_2 + C_1$	C_2	$\varepsilon C_4 + C_3$	C_4	$\varepsilon C_7 + C_5$	C_6	C_7	$C_8 - \varepsilon C_7$
C_8	C_1	$e^{\varepsilon}C_2$	$e^{-2\varepsilon}C_3$	$e^{-\varepsilon}C_4$	C_5	$e^{-2\varepsilon}C_6$	$e^{\varepsilon}C_7$	C_8

2.2.1 Solution of (2.2) *via* direct integration

Eq. (2.2) can be integrated to obtain the NLODE

$$\psi'^2 + \frac{2a}{3}\psi'^3 + \frac{c}{b}\psi'^2 + \frac{2k_0}{b} = 0, \tag{2.3}$$

where k_0 is a constant of integration. It is of convenience to set $\psi' = \mathcal{H}$, so that Eq. (2.3) becomes

$$\mathcal{H}'^2 = -\frac{2a}{3}\mathcal{H}^3 - \frac{c}{b}\mathcal{H}^2 - \frac{2k_0}{b}. \tag{2.4}$$

Assuming that the cubic polynomial equation

$$\frac{2a}{3}\mathcal{H}^3 + \frac{c}{b}\mathcal{H}^2 + \frac{2k_0}{b} = 0$$

has the real roots ε_1, ε_2, and ε_3 such that $\varepsilon_1 > \varepsilon_2 > \varepsilon_3$, Eq. (2.4) is expressed as

$$\mathcal{H}'^2 = -\frac{2a}{3}(\mathcal{H} - \varepsilon_1)(\mathcal{H} - \varepsilon_2)(\mathcal{H} - \varepsilon_3),$$

whose solution is [37,38]

$$\mathcal{H}(z) = \varepsilon_2 + (\varepsilon_1 - \varepsilon_2)\mathrm{cn}^2\left\{\sqrt{\frac{a(\varepsilon_1 - \varepsilon_3)}{6}}\, z \;|\mathcal{M}^2\right\}, \tag{2.5}$$
$$\mathcal{M}^2 = \frac{\varepsilon_1 - \varepsilon_2}{\varepsilon_1 - \varepsilon_3},$$

with cn being the Jacobi cosine elliptic function. Upon integration of Eq. (2.5) and then retrograding to original variables, the solution of the 2DKdV model (1.1) becomes

$$u(t,x,y) = \sqrt{\frac{6(\varepsilon_1 - \varepsilon_2)^2}{a(\varepsilon_1 - \varepsilon_3)\mathcal{M}^8}} \times\left\{\mathrm{EllipticE}\left[\mathrm{sn}\left(\frac{a(\varepsilon_1 - \varepsilon_3)}{6}z, \mathcal{M}^2\right), \mathcal{M}^2\right]\right\} + \left\{\varepsilon_2 - (\varepsilon_1 - \varepsilon_2)\frac{1 - \mathcal{M}^4}{\mathcal{M}^4}\right\}z + k_1, \tag{2.6}$$

where k_1 is a constant, $z = x + by + ct$, and $\mathrm{EllipticE}[q, v]$ represents the incomplete elliptic integral [39]

$$\mathrm{EllipticE}[q, v] = \int_0^v \sqrt{\frac{1 - v^2n^2}{1 - n^2}}\, dn.$$

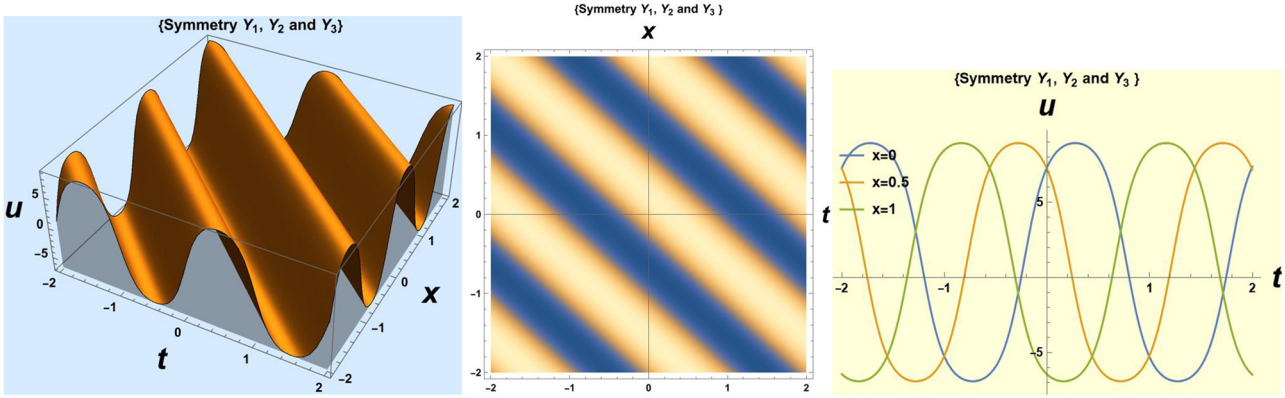

Figure 1: (a) 3D plot depicting the periodic soliton solution (2.6) for the parameter values $\varepsilon_1 = 10$, $\varepsilon_2 = 5$, $\varepsilon_3 = 3$, $k_1 = 1$, $a = 4$, $b = 2$, $c = 0.9$, $y = 1$, $-2 \le t, x \le 2$, (b) 2D density plot, and (c) 2D graph of solution (2.6), $-2 \le t \le 2$.

Figure 1 illustrates the wave profile of the periodic solution (2.6) under specific parametric assignments.

2.2.2 Special cases of elliptic function solution

It is a well-established fact that special limits of the Jacobi elliptic function can yield other mathematical functions, including hyperbolic and trigonometric functions. Leveraging this concept, we aim to obtain more solutions of (1.1) derived from the established Jacobi elliptic solution (2.5). Specifically, considering the range $0 \le \mathcal{M}^2 \le 1$, we investigate two cases: $\mathcal{M}^2 \to 1$ and $\mathcal{M}^2 \to 0$, which, respectively, lead to hyperbolic and trigonometric solutions

$$\mathcal{H}(z) = \varepsilon_2 + (\varepsilon_1 - \varepsilon_2)\,\mathrm{sech}^2\left(\sqrt{\frac{a(\varepsilon_1 - \varepsilon_3)}{6}}\,z\right),$$

$$\mathcal{H}(z) = \varepsilon_2 + (\varepsilon_1 - \varepsilon_2)\cos^2\left(\sqrt{\frac{a(\varepsilon_1 - \varepsilon_3)}{6}}\,z\right).$$

Upon integration of these solutions with respect to z, we obtain the following expressions:

$$u(t,x,y) = \frac{\sqrt{6}\,(\varepsilon_1 - \varepsilon_2)}{\sqrt{a(\varepsilon_1 - \varepsilon_3)}}\tanh\left(\sqrt{\frac{a(\varepsilon_1 - \varepsilon_3)}{6}}\,z\right) + \varepsilon_2 z + k_1, \tag{2.7}$$

$$u(t,x,y) = \frac{(\varepsilon_1 - \varepsilon_2)\left\{2z\sqrt{a(\varepsilon_1 - \varepsilon_3)} + \sqrt{6}\,\sin\left(\sqrt{\frac{2}{3}}\,z\sqrt{a(\varepsilon_1 - \varepsilon_3)}\right)\right\}}{4\sqrt{a(\varepsilon_1 - \varepsilon_3)}} + \varepsilon_2 z + k_1, \tag{2.8}$$

respectively, where $z = x + by + ct$. The wave profiles of solution (2.7) and (2.8) are given in Figures 2 and 3.

2.2.3 Special case of (2.3)

We derive a solution of the underlying model (1.1) by considering the case $k_0 = 0$ in Eq. (2.3), which gives us the NLODE

$$\psi''^2 + \frac{2a}{3}\psi'^3 + \frac{c}{b}\psi'^2 = 0.$$

Integration of the resultant NLODE gives

$$u(t,x,y) = a_2 - \frac{3\sqrt{c}}{a\sqrt{b}}\tan\left\{\frac{\sqrt{c}\,(x + by + ct)}{2\sqrt{b}} \pm \frac{1}{2}\sqrt{3c}\,a_1\right\}, \tag{2.9}$$

where a_1 and a_2 are the constants of integration (Figure 4).

2.2.4 Solution of (1.1) *via* Kudryashov's method

We note that Eq. (2.2) can be solved using Kudryashov's approach as illustrated in the study by Kudryashov [40]. To achieve this, it is assumed that the solution of Eq. (2.2) takes the form

$$\psi(z) = \sum_{i=0}^{\mathfrak{N}} \mathfrak{B}_i \mathfrak{M}^i(z), \tag{2.10}$$

where $\mathfrak{B}_i$ $(i = 0, 1, 2, \ldots, \mathfrak{N})$ are the constants, $\mathfrak{N}$ is a positive integer obtained through the balancing procedure, and $\mathfrak{M}(z)$ solves the Riccati equation

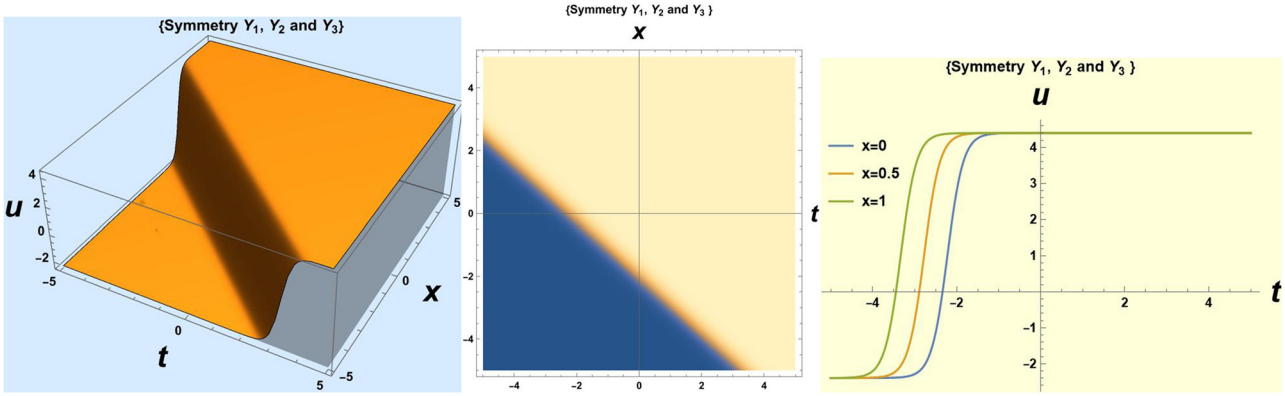

Figure 2: (a) 3D plot depicting the kink-shaped soliton solution (2.7) for the parameter values $\varepsilon_1 = 10$, $\varepsilon_2 = 0$, $\varepsilon_3 = -3$, $k_1 = 1$, $a = 4$, $b = 2$, $c = 0.9$, $y = 1$, over the interval $-5 \le t, x \le 5$, (b) 2D density plot illustrates solution (2.7), and (c) 2D graph of solution (2.7) for the interval $-5 \le t \le 5$.

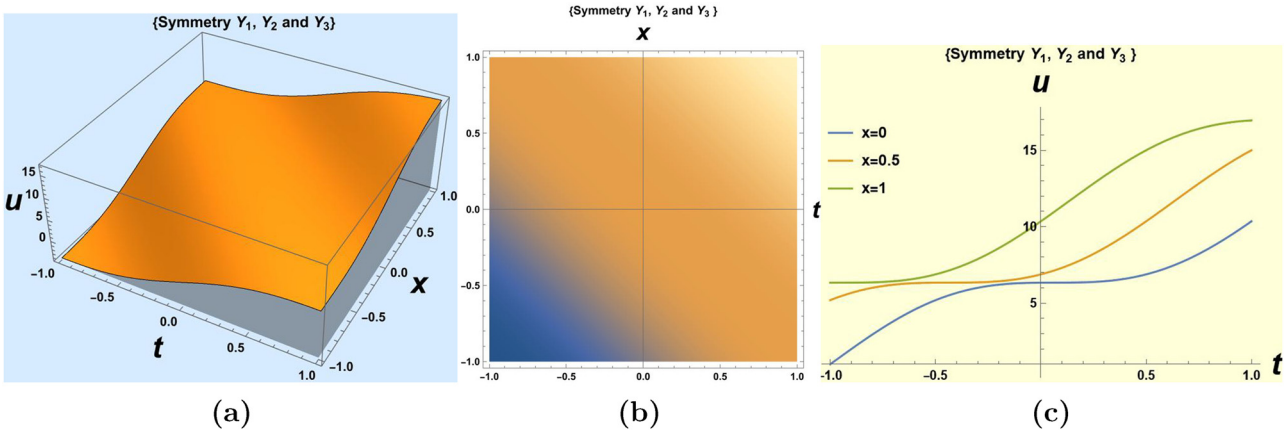

Figure 3: (a) 3D plot illustrating the periodic soliton solution (2.8) for the parameter values $\varepsilon_1 = 10$, $\varepsilon_2 = 0$, $\varepsilon_3 = -3$, $k_1 = 1$, $\alpha = 1$, $b = 2$, $c = 1$, $y = 1$, over the interval $-1 \le t, x \le 1$, (b) 2D density plot depicting solution (2.8), and (c) 2D graph of solution (2.8) over the interval $-1 \le t \le 1$.

$$\mathfrak{M}'(z) = \mathfrak{M}^2(z) - \mathfrak{M}(z), \tag{2.11}$$

whose solution is given by [40]

$$\mathfrak{M}(z) = \frac{1}{1 + e^z}. \tag{2.12}$$

For Eq. (2.2), balancing the terms ψ''' and ψ'^2, we obtain $\mathfrak{N} = 1$, hence we have

$$\psi(z) = \mathfrak{B}_0 + \mathfrak{B}_1\mathfrak{M}(z). \tag{2.13}$$

Substituting Eq. (2.13) into (2.2) and using (2.11), we obtain an algebraic equation

$$\begin{aligned}&\alpha\mathfrak{B}_1^2 b\mathfrak{M}^4(z) - 2\alpha\mathfrak{B}_1^2 b\mathfrak{M}^3(z)\\ &\quad + \alpha\mathfrak{B}_1^2 b\mathfrak{M}^2(z) + 6\mathfrak{B}_1 b\mathfrak{M}^4(z) - 12\mathfrak{B}_1 b\mathfrak{M}^3(z)\\ &\quad + 7\mathfrak{B}_1 b\mathfrak{M}^2(z) + \mathfrak{B}_1 b\mathfrak{M}(z) + \mathfrak{B}_1 c\mathfrak{M}(z)^2 - \mathfrak{B}_1 c\mathfrak{M}(z) = 0,\end{aligned}$$

which upon splitting on powers of $\mathfrak{M}(z)$ leads to the system

$$\begin{aligned}&\mathfrak{B}_1 b + \mathfrak{B}_1 c = 0,\\ &\alpha\mathfrak{B}_1^2 b + 7\mathfrak{B}_1 b + \mathfrak{B}_1 c = 0,\\ &\alpha\mathfrak{B}_1^2 b + 6\mathfrak{B}_1 b = 0,\end{aligned}$$

which can be solved to obtain

$$\mathfrak{B}_0 = \mathfrak{B}_0, \mathfrak{B}_1 = -\frac{6}{\alpha}, b = -c. \tag{2.14}$$

Therefore, reverting to the t, x, and y variables, one obtains the general solution of the 2DKdV model (1.1) corresponding to the constants (2.14) to be

$$u(t, x, y) = \mathfrak{B}_0 - \frac{6}{\alpha\{1 + e^{x+b(y-t)}\}}, \tag{2.15}$$

where $\mathfrak{B}_0$ is a constant. The wave profile corresponding to the exponential solution is depicted in Figure 5.

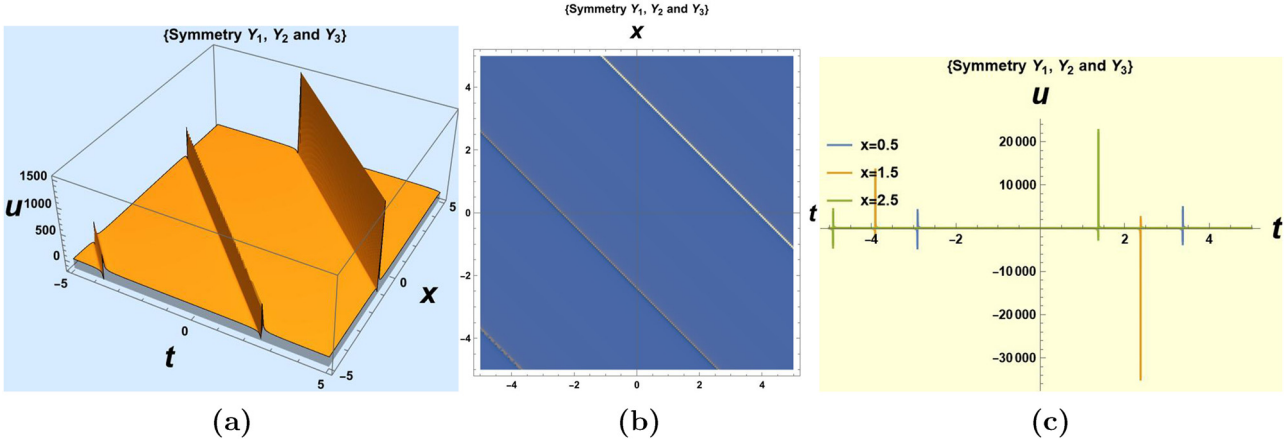

Figure 4: (a) 3D plot illustrating the solution (2.9) for the parametric values $a_1 = 1$, $a_2 = 1$, $\alpha = 1$, $b = 1$, $c = 1$, $y = 1$, over the interval $-5 \le t, x \le 5$, (b) 2D density plot depicts solution (2.9), and (c) 2D graph of solution (2.9) shown for the interval $-5 \le t \le 5$.

2.2.5 Solution by the simplest equation method

In our pursuit of solving the NLODE (2.2), we employ the approach known as the simplest equation method, as detailed in works [41,42]. Subsequently, we obtain solutions for the 2DKdV model (1.1). This method entails the utilization of the Bernoulli equation and the Riccati equation, which are

$$\mathfrak{f}'(z) = l\mathfrak{f}(z) + n\mathfrak{f}^2(z) \tag{2.16}$$

and

$$\mathfrak{f}'(z) = l\mathfrak{f}^2(z) + n\mathfrak{f}(z) + s, \tag{2.17}$$

where l, n, and s are the constants. We ascertain solutions of Eq. (2.2) in the format

$$\psi(z) = \sum_{i=0}^{\mathfrak{n}} \mathfrak{a}_i(\mathfrak{f}(z))^i, \tag{2.18}$$

where $\mathfrak{f}$ solves the Bernoulli Eq. (2.16) or the Riccati Eq. (2.17). Here, $\mathfrak{n}$ represents a positive integer whose value is obtained through the balancing procedure, and $\mathfrak{a}_0, \ldots, \mathfrak{a}_{\mathfrak{n}}$ are the constants. The solutions of the Bernoulli Eq. (2.16) that are used here are

$$\mathfrak{f}(z) = \left\{\frac{-lc_1}{n(c_1 + \cosh[l(z + c_0)] - \sinh[l(z + c_0)])}\right\} \tag{2.19}$$

and

$$\mathfrak{f}(z) = \left\{\frac{-l(\cosh[l(z + c_0)] + \sinh[l(z + c_0)])}{n(c_2 + \cosh[l(z + c_0)] + \sinh[l(z + c_0)])}\right\}, \tag{2.20}$$

where c_0, c_1, and c_2 are the constants. For the Riccati Eq. (2.17), we consider the solutions

$$\mathfrak{f}(z) = -\frac{n}{2l} - \frac{\theta}{2l}\tanh\left\{\frac{1}{2}\theta(z + c_0)\right\} \tag{2.21}$$

and

$$\mathfrak{f}(z) = -\frac{n}{2l} - \frac{\theta}{2l}\tanh\left(\frac{1}{2}\theta z\right) + \frac{\operatorname{sech}\left(\frac{\theta z}{2}\right)}{c_0\cosh\left(\frac{\theta z}{2}\right) - \frac{2l}{\theta}\sinh\left(\frac{\theta z}{2}\right)}, \tag{2.22}$$

with $\theta = \sqrt{n^2 - 4ls}$ and c_0 being a constant.

2.2.5.1 Bernoulli case

Applying the balancing procedure, we obtain $\mathfrak{n} = 1$. This leads to Eq. (2.18) taking the form

$$\psi(z) = \mathfrak{a}_0 + \mathfrak{a}_1\mathfrak{f}(z). \tag{2.23}$$

By substituting (2.23) into (2.2) and making use of the Bernoulli Eq. (2.16), we obtain

$$\begin{aligned}&\mathfrak{a}_1 bl^3\mathfrak{f} + 7\mathfrak{a}_1 bl^2 n\mathfrak{f}^2 + \alpha\mathfrak{a}_1^2 bl^2\mathfrak{f}^2 + 12\mathfrak{a}_1 bln^2\mathfrak{f}^3 + 2\alpha\mathfrak{a}_1^2 bln\mathfrak{f}^3\\ &+ 6\mathfrak{a}_1 bn^3\mathfrak{f}^4 + \alpha\mathfrak{a}_1^2 bn^2\mathfrak{f}^4 + \mathfrak{a}_1 cl\mathfrak{f} + \mathfrak{a}_1 cn\mathfrak{f}^2 = 0,\end{aligned}$$

whereby equating the coefficients of $\mathfrak{f}^i$ to zero leads to

$$\begin{aligned}&\mathfrak{a}_1 bl^3 + \mathfrak{a}_1 cl = 0,\\ &\alpha\mathfrak{a}_1^2 bl^2 + 7\mathfrak{a}_1 bl^2 n + \mathfrak{a}_1 cn = 0,\\ &6\mathfrak{a}_1 bln^2 + \alpha\mathfrak{a}_1^2 bln = 0,\\ &6\mathfrak{a}_1 bn^3 + \alpha\mathfrak{a}_1^2 bn^2 = 0.\end{aligned}$$

Solving the aforementioned system, one obtains

$$\mathfrak{a}_0 = \mathfrak{a}_0, \quad \mathfrak{a}_1 = -\frac{6n}{\alpha}, \quad b = -\frac{c}{l^2}.$$

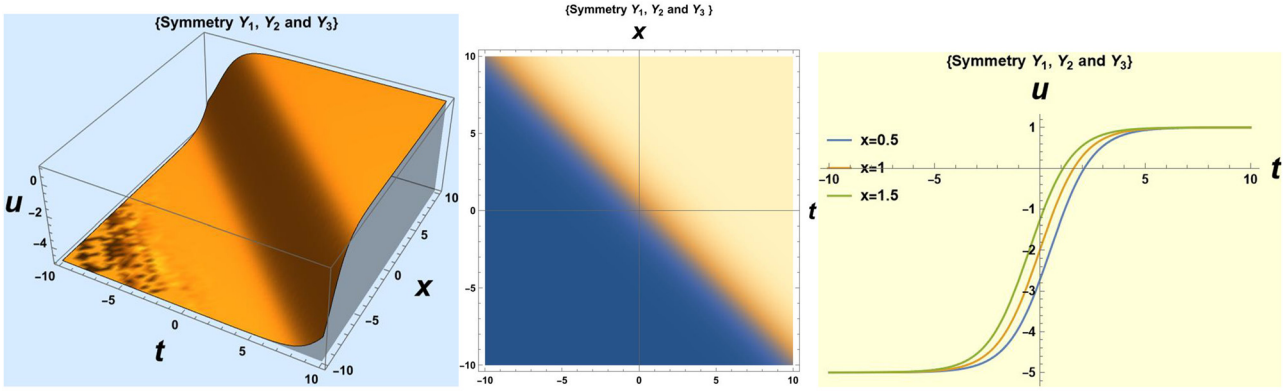

Figure 5: (a) 3D plot depicting the kink-shaped soliton solution (2.15) for the following parameter values: $\alpha = 1$, $c = 1$, and $\mathfrak{B}_0 = 1$, over the interval $-10 \le t, x \le 10$, (b) 2D density plot illustrates solution (2.15), and (c) 2D plot of solution (2.15) on the interval $-10 \le t \le 10$.

Therefore, solutions to the 2DKdV Eq. (1.1) are

$$u(t,x,y) = \mathfrak{a}_0 + \frac{6lc_1}{\alpha(\cosh(l(c_0+z)) - \sinh(l(c_0+z)) + c_1)}, \tag{2.24}$$

$$u(t,x,y) = \mathfrak{a}_0 + \frac{6l(\sinh(l(c_0+z)) + \cosh(l(c_0+z)))}{\alpha(\sinh(l(c_0+z)) + \cosh(l(c_0+z)) + c_2)}, \tag{2.25}$$

where $z = x + by + ct$ and c_0, c_1, and c_2 are the arbitrary constants. The wave profiles of solutions (2.24) and (2.25) are provided in Figures 6 and 7, respectively.

2.2.5.2 Riccati case

Note that the Riccati case follows a procedure similar to that of the Bernoulli case, which involves the incorporation of the expression for $\psi(z)$ into Eq. (2.2) and utilization of the Riccati Eq. (2.17). This leads to the derivation of an algebraic equation

$$\begin{aligned}&6\mathfrak{a}_1 bl^3\mathfrak{f}^4 + 12\mathfrak{a}_1 bl^2 n\mathfrak{f}^3 + 8\mathfrak{a}_1 bl^2 s\mathfrak{f}^2 + \alpha\mathfrak{a}_1^2 bl^2\mathfrak{f}^4 + 7\mathfrak{a}_1 bln^2\mathfrak{f}^2\\ &+ 8\mathfrak{a}_1 blns\mathfrak{f} + 2\alpha\mathfrak{a}_1^2 bln\mathfrak{f}^3 + 2\alpha\mathfrak{a}_1^2 bls\mathfrak{f}^2 + 2\mathfrak{a}_1 bls^2 + \mathfrak{a}_1 bn^3\mathfrak{f}\\ &+ \alpha\mathfrak{a}_1^2 bn^2\mathfrak{f}^2 + \mathfrak{a}_1 bn^2 s + 2\alpha\mathfrak{a}_1^2 bns\mathfrak{f} + \alpha\mathfrak{a}_1^2 bs^2 + \mathfrak{a}_1 cl\mathfrak{f}^2\\ &+ \mathfrak{a}_1 cn\mathfrak{f} + \mathfrak{a}_1 cs = 0,\end{aligned}$$

which when splat on powers of $\mathfrak{f}$ gives the algebraic system of equations

$$\begin{aligned}&2\mathfrak{a}_1 bls^2 + \mathfrak{a}_1 bn^2 s + \alpha\mathfrak{a}_1^2 bs^2 + \mathfrak{a}_1 cs = 0,\\ &8\mathfrak{a}_1 blns + \mathfrak{a}_1 bn^3 + 2\alpha\mathfrak{a}_1^2 bns + \mathfrak{a}_1 cn = 0,\\ &8\mathfrak{a}_1 bl^2 s + 7\mathfrak{a}_1 bln^2 + 2\alpha\mathfrak{a}_1^2 bls + \alpha\mathfrak{a}_1^2 bn^2 + \mathfrak{a}_1 cl = 0,\\ &6\mathfrak{a}_1 bl^2 n + \alpha\mathfrak{a}_1^2 bln = 0,\\ &6\mathfrak{a}_1 bl^3 + \alpha\mathfrak{a}_1^2 bl^2 = 0,\end{aligned}$$

which is solved with the aid of Mathematica to obtain $\mathfrak{a}_0$ and $\mathfrak{a}_1$ as

$$\mathfrak{a}_0 = \mathfrak{a}_0, \quad \mathfrak{a}_1 = -\frac{6l}{\alpha}, \quad b = -\frac{c}{n^2 - 4ls}.$$

Thus, the solutions of the 2DKdV equation are

$$\begin{aligned}u(t,x,y) = \mathfrak{a}_0 + \frac{3}{\alpha}\Bigg(&\sqrt{n^2-4ls}\,\tanh\Bigg(\frac{1}{2}(c_0\\ &+ z)\sqrt{n^2-4ls}\Bigg) + n\Bigg),\end{aligned} \tag{2.26}$$

$$\begin{aligned}u(t,x,y) = \mathfrak{a}_0 + \frac{3n}{\alpha}&\\ - \frac{6l\sqrt{n^2-4ls}\,\operatorname{sech}^2\left(\frac{1}{2}z\sqrt{n^2-4ls}\right)}{\alpha c_0\sqrt{n^2-4ls} - 2\alpha l\tanh\left(\frac{1}{2}z\sqrt{n^2-4ls}\right)}&\\ + \frac{3\sqrt{n^2-4ls}}{\alpha}\tanh\left(\frac{1}{2}z\sqrt{n^2-4ls}\right),&\end{aligned} \tag{2.27}$$

where $z = x + by + ct$ and c_0 is an arbitrary constant. The temporal evolution of the wave profiles for the solutions presented in Eqs. (2.26) and (2.27) is depicted in Figures 8 and 9, respectively.

Reduction 2. We consider the symmetry $C_5 = t\partial/\partial t + y\partial/\partial y$. In this case, we obtain the invariants

$$u = \mathcal{F}(x,z), z = \frac{y}{t},$$

that when inserted into the model (1.1) gives the NLPDE

$$\alpha\mathcal{F}_x\mathcal{F}_z + \mathcal{F}_{xxz} - z\mathcal{F}_z = 0. \tag{2.28}$$

Further investigation *via* Lie group analysis of Eq. (2.28) yields four Lie point symmetries

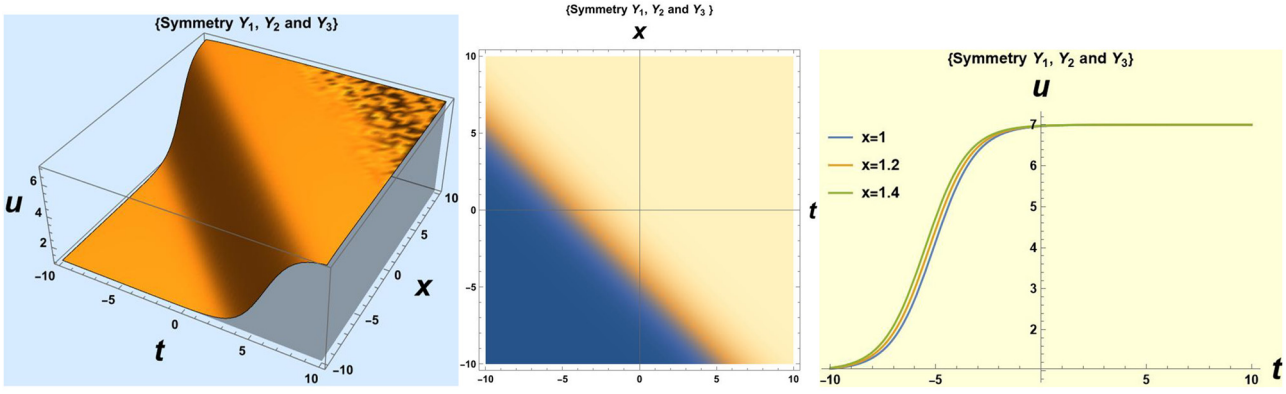

(a) (b) (c)

Figure 6: (a) 3D graph showing kink-shaped solution (2.24) for the parameters $\mathfrak{a}_0 = 1$, $\alpha = 1$, $l = 1$, $c = 1$, $c_0 = 4$, $c_1 = 3$, $y = 1$, $-10 \le t, x \le 10$, (b) density plot, and (c) 2D graph for interval $-10 \le t \le 10$.

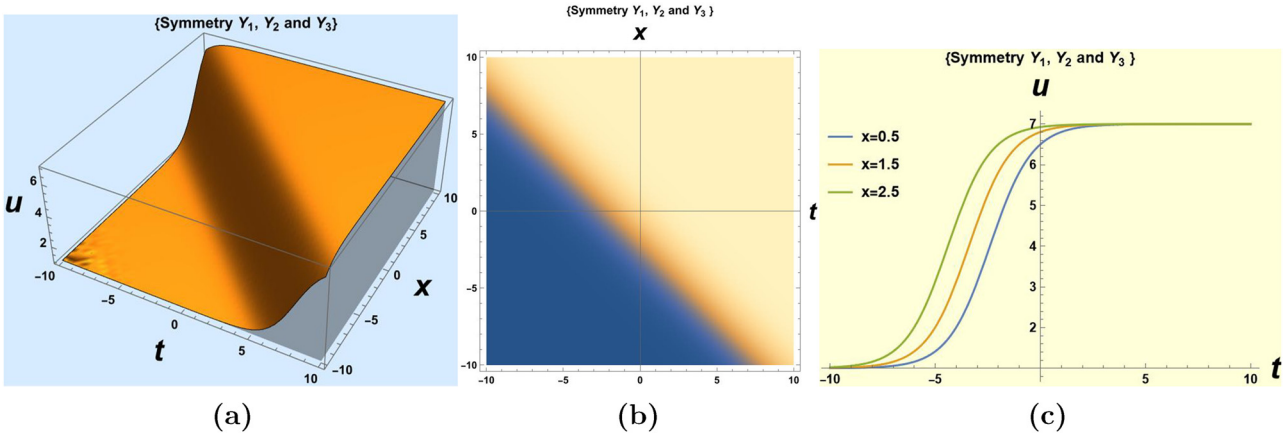

(a) (b) (c)

Figure 7: (a) 3D plot displaying the kink-shaped solution (2.25) for the values $\alpha = 1$, $l = 1$, $\mathfrak{a}0 = 1$, $c = 1$, $c_0 = 4$, $c2 = 1$, $y = 1$, over the range $-10 \le t, x \le 10$, (b) 2D density plot, and (c) 2D graph over the range $-10 \le t \le 10$.

$$\mathcal{J}_1 = \frac{\partial}{\partial x}, \quad \mathcal{J}_2 = \frac{\partial}{\partial \mathcal{F}},$$
$$\mathcal{J}_3 = \alpha\frac{\partial}{\partial z} + x\frac{\partial}{\partial \mathcal{F}}, \quad \mathcal{J}_4 = x\frac{\partial}{\partial x} - 2z\frac{\partial}{\partial z} - \mathcal{F}\frac{\partial}{\partial \mathcal{F}}.$$

When we utilize the symmetry $\mathcal{J}_1$, we obtain $u(t, x, y) = \mathfrak{c}_1$, where $\mathfrak{c}_1$ is a constant of integration. Symmetry $\mathcal{J}_2$ yields no result. On the other hand, engaging $\mathcal{J}_3$, we obtain

$$\mathcal{F} = \frac{xz}{\alpha} + \mathfrak{P}(x),$$

which transforms (2.28) to the first-order ordinary differential equation $\mathfrak{P}' = 0$. Solving this and retrograding to original variables, we obtain

$$u(t, x, y) = \frac{xy}{\alpha t} + \nu, \tag{2.29}$$

where ν is a constant. The solution profile of (2.29) is shown in Figure 10.

Moreover, from the symmetry $\mathcal{J}_4$, we have $\mathcal{F} = \frac{1}{x}\mathfrak{U}(p)$ with $p = x^2 z$, which reduces (2.28) into the NLODE

$$4p^2\mathfrak{U}''' - \alpha\mathfrak{U}'\mathfrak{U} + 2\alpha p\mathfrak{U}'^2 - p\mathfrak{U}' + 6p\mathfrak{U}'' = 0. \tag{2.30}$$

We note that the aforementioned equation is solvable by the power series solution method.

2.2.5.3 Solution of (2.30) by the power series method

The power series solution technique proves advantageous in finding solutions of intricate NLODEs [43], as exemplified by Eq. (2.30). Commencing the analysis, consider representing the solution to Eq. (2.30) in the manner

$$\mathfrak{U}(p) = \sum_{\tau=0}^{\infty} \mathfrak{e}_\tau p^\tau, \tag{2.31}$$

where $\mathfrak{e}_\tau (\tau \ge 0)$ are the constants. Inserting (2.31) into (2.30) leads to

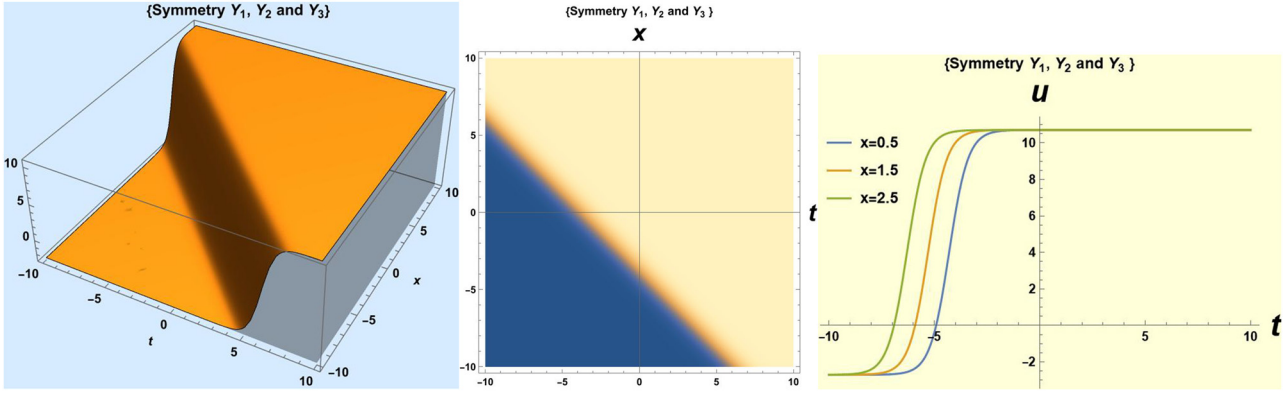

(a) (b) (c)

Figure 8: (a) 3D plot illustrating the kink-shaped solution (2.26) for the parameter values $\alpha = 1$, $l = -1$, $\mathfrak{a}_0 = 1$, $c = 1$, $n = 1$, $s = 1$, $c_0 = 4$, and $y = 1$, over the range $-10 \le t, x \le 10$, (b) 2D density plot, and (c) 2D graph of depicted over the interval $-10 \le t \le 10$.

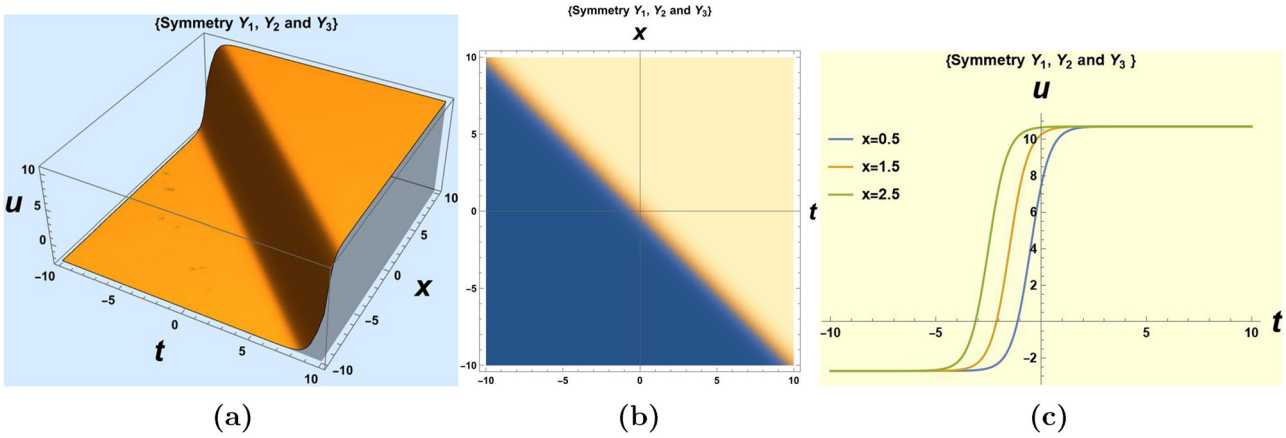

(a) (b) (c)

Figure 9: 3D plot depicting the kink-shaped solution (2.27) with the specified parameter values $\alpha = 1$, $l = -1$, $a_0 = 1$, $c = 1$, $n = 1$, $s = 1$, $c_0 = 4$, and $y = 1$, over the range $-10 \le t, x \le 10$, (b) 2D density plot and (c) 2D graph depicted over the interval $-10 \le t \le 10$.

$$
\begin{aligned}
&4\sum_{\tau=2}^{\infty}\tau(\tau-1)(\tau+1)\epsilon_{\tau+1}p^{\tau}\\
&-\alpha\sum_{\tau=2}^{\infty}\left[\sum_{i=0}^{\tau}(\tau-i+1)\epsilon_i\epsilon_{\tau-i+1}\right]p^{\tau}\\
&+2\alpha\sum_{\tau=2}^{\infty}\left[\sum_{i=0}^{\tau}\tau(\tau-i+1)\epsilon_i\epsilon_{\tau-i+1}\right]p^{\tau}\\
&-\sum_{\tau=2}^{\infty}\tau\epsilon_{\tau}p^{\tau}+6\sum_{\tau=2}^{\infty}\tau(\tau+1)\epsilon_{\tau+1}p^{\tau}=0,
\end{aligned}
\tag{2.32}
$$

whereby it is easy to note that

$$2\alpha\epsilon_1\epsilon_2+12\epsilon_2-\epsilon_1=0, \quad \text{for} \quad \tau=1. \tag{2.33}$$

Consequently, for $\tau \ge 2$, the recursion relation is given by

$$
\begin{aligned}
\epsilon_{\tau+4}=\frac{1}{4\tau(\tau-1)(\tau+1)}\Big[&\tau\epsilon_{\tau}+6\tau(\tau+1)\epsilon_{\tau+1}\\
&+\sum_{i=0}^{\tau}(\tau-i+1)\epsilon_i\epsilon_{\tau-i+1}-2\alpha\sum_{i=0}^{\tau}\tau(\tau-i\\
&+1)\epsilon_i\epsilon_{\tau-i+1}\Big].
\end{aligned}
\tag{2.34}
$$

By employing the recursive relationship (2.34), one can systematically derive additional successive terms ϵ_{τ}, $(\tau \ge 2)$ within the power series expansion (2.31). It is pertinent to note that establishing the convergence of the aforementioned power series (2.31), characterized by coefficients outlined in (2.33) and (2.34), constitutes a straightforward

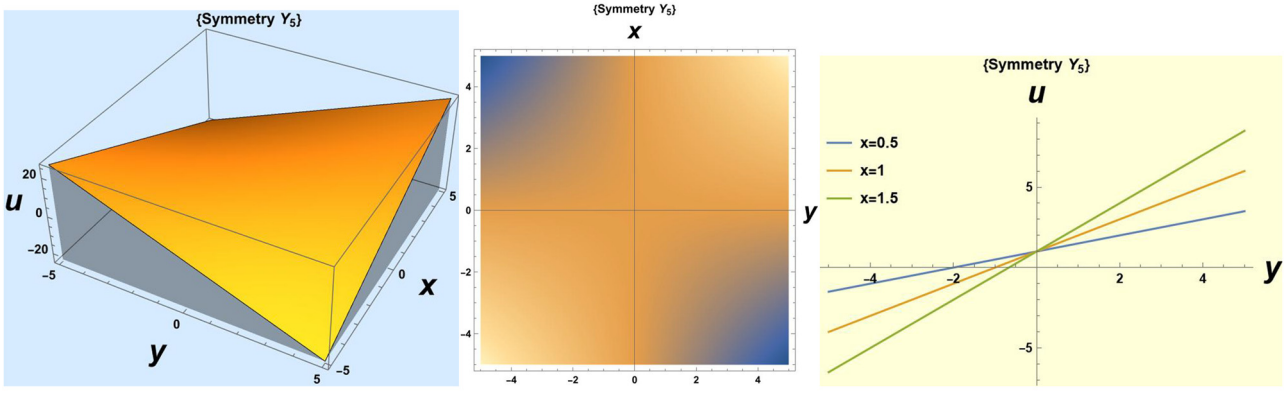

(a) (b) (c)

Figure 10: (a) 3D plot showing the solution (2.29) for the values $\alpha = 1$, $\nu = 1$ and $t = 1$, over the interval $-5 \le y, x \le 5$, (b) 2D density plot of solution (2.29), and (c) 2D plot of solution (2.29) depicted on the interval $-5 \le y \le 5$.

endeavour, as discussed in the study by Liu *et al.* [43]. For the sake of conciseness, the proof is omitted here. The solution to the NLODE (2.30) can thus be succinctly expressed as

$$\begin{aligned}\mathfrak{U}(p) &= \mathfrak{e}_0 + \mathfrak{e}_1 p + \frac{\mathfrak{e}_1}{2(6+\alpha\mathfrak{e}_1)}p^2 + \sum_{\mathfrak{r}=2}^{\infty}\frac{1}{4\mathfrak{r}(\mathfrak{r}-1)(\mathfrak{r}+1)} \\ &\times\left[6\mathfrak{r}(\mathfrak{r}+1)\mathfrak{e}_{\mathfrak{r}+1} + \mathfrak{r}\mathfrak{e}_{\mathfrak{r}} + \sum_{i=0}^{\mathfrak{r}}(\mathfrak{r}-i+1)\mathfrak{e}_i\mathfrak{e}_{\mathfrak{r}-i+1}\right. \\ &\left. - 2\alpha\sum_{i=0}^{\mathfrak{r}}\mathfrak{r}(\mathfrak{r}-i+1)\mathfrak{e}_i\mathfrak{e}_{\mathfrak{r}-i+1}\right]p^{\mathfrak{r}+1}.\end{aligned}$$

Hence, reverting to the original variables, we obtain

$$\begin{aligned}u(t,x,y) = x^{-1}\Bigg[&\mathfrak{e}_0 + \mathfrak{e}_1\left(\frac{x^2y}{t}\right) + \frac{\mathfrak{e}_1}{2(6+\alpha\mathfrak{e}_1)}\left(\frac{x^2y}{t}\right)^2 \\ &+ \sum_{\mathfrak{r}=2}^{\infty}\frac{1}{4\mathfrak{r}(\mathfrak{r}-1)(\mathfrak{r}+1)}\{6\mathfrak{r}(\mathfrak{r}+1)\mathfrak{e}_{\mathfrak{r}+1} \\ &+ \mathfrak{r}\mathfrak{e}_{\mathfrak{r}} + \sum_{i=0}^{\mathfrak{r}}(\mathfrak{r}-i+1)\mathfrak{e}_i\mathfrak{e}_{\mathfrak{r}-i+1} \\ &- 2\alpha\sum_{i=0}^{\mathfrak{r}}\mathfrak{r}(\mathfrak{r}-i+1)\mathfrak{e}_i\mathfrak{e}_{\mathfrak{r}-i+1}\Bigg\}\left(\frac{x^2y}{t}\right)^{\mathfrak{r}+1}\Bigg],\end{aligned} \tag{2.35}$$

which is the power series solution to the 2DKdV model (1.1). We present the wave profile of the semi-analytical solution (2.35) in Figure 11.

Reduction 3. The infinitesimal symmetry $C_6 = at\partial/\partial t + x\partial/\partial u$ leads to invariant solution $u = xy/at + \mathcal{U}(t,x)$ that reduces the 2DKdV model (1.1) to $t\mathcal{U}_t + x\mathcal{U}_x = 0$. The solution to the partial differential equation (PDE) is given by $\mathcal{U} = \mathfrak{c}_1(x/t)$, where $\mathfrak{c}_1$ is a constant. Therefore, the solution of the 2DKdV Eq. (1.1) is

$$u(t,x,y) = \frac{xy}{at} + \mathfrak{c}_1\left(\frac{x}{t}\right). \tag{2.36}$$

We give the wave profile to the rational solution (2.36) in Figure 12.

Reduction 4. Invoking the symmetry $C_7 = at\partial/\partial t + y\partial/\partial u$, we obtain the invariant solution $u = xy/at + \mathfrak{F}(t,x)$ that transforms model (1.1) to the PDE $t\mathfrak{F}_t + y\mathfrak{F}_y = 0$. This PDE has the solution $\mathfrak{F} = k(y/t)$, where k is an integration constant. Consequently, we obtain that the solution of the 2DKdV model (1.1) is

$$u(t,x,y) = \frac{xy}{at} + k\left(\frac{y}{t}\right). \tag{2.37}$$

The wave profile to the rational solution (2.37) can be viewed in Figure 13.

Reduction 5. Finally, we engage the symmetry $C_8 = x\partial/\partial x - 2y\partial/\partial y - u\partial/\partial u$. To this end, we obtain the invariant solution

$$u = \frac{1}{x}U(t,s), \quad s = x^2y,$$

which when substituted into the 2DKdV model (1.1) gives the NLPDE

$$U_t - aU_sU + 2asU_s^2 + 4s^2U_{sss} + 6sU_{ss} = 0. \tag{2.38}$$

Eq. (2.38) admits two infinitesimal symmetries

$$\mathcal{P}_1 = \frac{\partial}{\partial t}, \quad \mathcal{P}_3 = t\frac{\partial}{\partial t} + s\frac{\partial}{\partial s}.$$

Symmetry $\mathcal{P}_1$ gives the group-invariant solution $U = \mathcal{G}(s)$, which further reduces (2.38) to

$$4s^2\mathcal{G}''' - a\mathcal{G}'\mathcal{G}(s) + 2as\mathcal{G}'^2 + 6s\mathcal{G}'' = 0. \tag{2.39}$$

Observe that the NLODE (2.39) exhibits a form similar to that of Eq. (2.30), thereby suggesting its amenable solution through the power series method in a manner analogous to

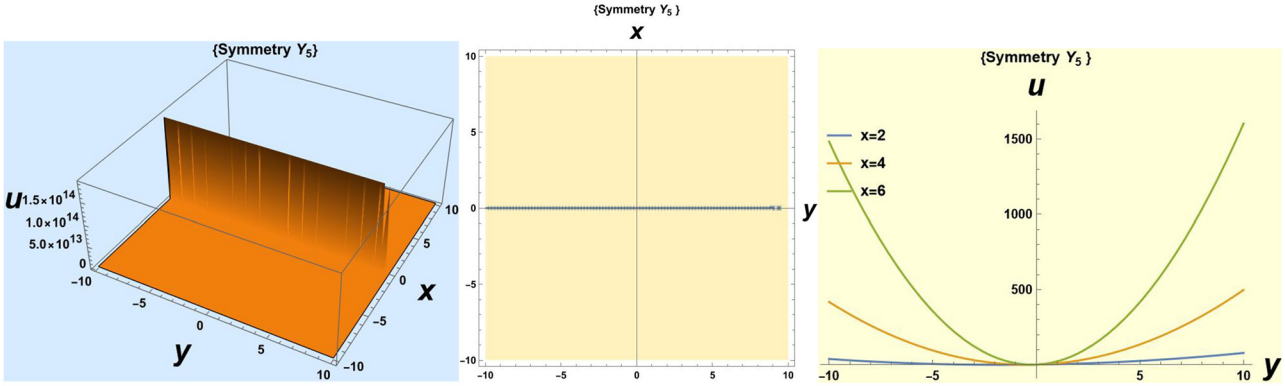

Figure 11: (a) 3D plot of power series solution (2.35) for parameters $\alpha = 1$, $\mathfrak{e}_0 = 1$, $\mathfrak{e}_1 = 1$, for interval $-10 \le y, x \le 10$, (b) 2D density plot, and (c) 2D graph for the range $-10 \le y \le 10$.

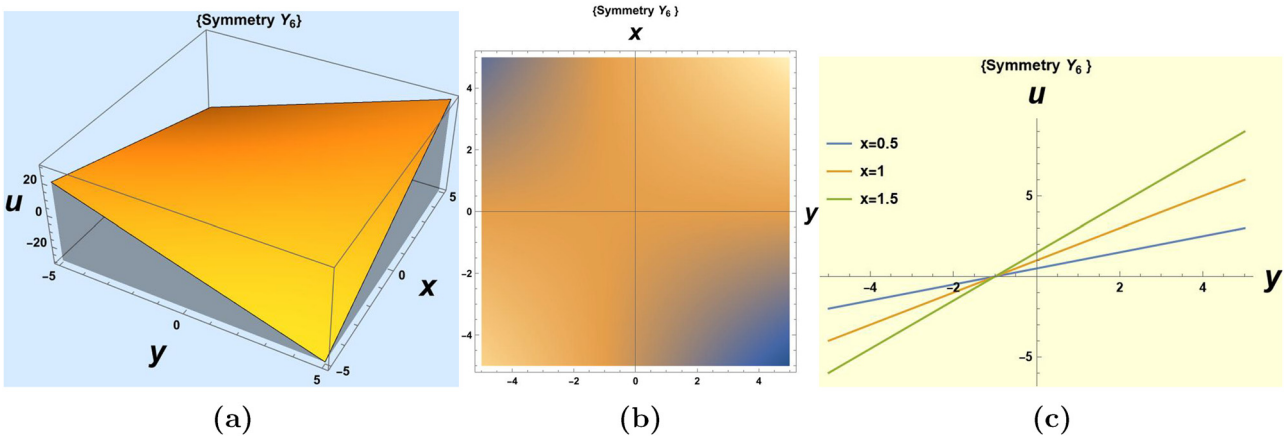

Figure 12: (a) 3D plot showing the solution (2.36) for the parameter values $\alpha = 1$, $c_1 = 1$, and $t = 1$, over the interval $-5 \le y, x \le 5$, (b) 2D density plot of solution (2.36), and (c) 2D plot of solution (2.36) depicted on the interval $-5 \le y \le 5$.

the latter, which we omit here. Engaging symmetry $\mathcal{P}_2$ in the same manner yields

$$U = Q(q), q = \frac{s}{t}, \tag{2.40}$$

which transforms (2.38) to the NLODE

$$4q^2Q''' - \alpha Q'Q(q) + 2\alpha qQ'^2 - qQ' + 6qQ'' = 0. \tag{2.41}$$

Note that this NLODE is similar to Eq. (2.30) whose solution has already been provided.

3 Graphical depiction and application of results

This section presents the graphical representation of the soliton solutions obtained for the 2DKdV model (1.1), covering kink, singular, and periodic solitons, as outlined in (2.6), (2.7), (2.8), (2.9), (2.15), (2.24), (2.25), (2.26), and (2.27). The results are illustrated using both 3D and 2D structures to highlight the model's features. To visualize the physical behaviour of the model, we depict the soliton structures by assigning suitable values to the relevant parameters. Specifically, the dynamics of the periodic soliton solution (2.6) are illustrated through 3D plots, contour plots, and 2D projections in Figure 1, with varying parameter values $\varepsilon_1 = 10$, $\varepsilon_2 = 5$, $\varepsilon_3 = 3$, $k_1 = 1$, $\alpha = 4$, $b = 2$, $c = 0.9$, and fixed values $y = 1$, and $-2 \le t, x \le 2$. Additionally, we investigate the dynamics of the kink-shaped solitary wave solution (2.7) by presenting Figure 2 with different parameter values $\varepsilon_1 = 10$, $\varepsilon_2 = 0$, $\varepsilon_3 = -3$, $k_1 = 1$, $\alpha = 4$, $b = 2$, and $c = 0.9$, where $y = 1$, and $-5 \le t, x \le 5$. Following this, the periodic soliton solution (2.8) is illustrated through 3D, density, and 2D plots in Figure 3, with varying parameter values $\varepsilon_1 = 10$,

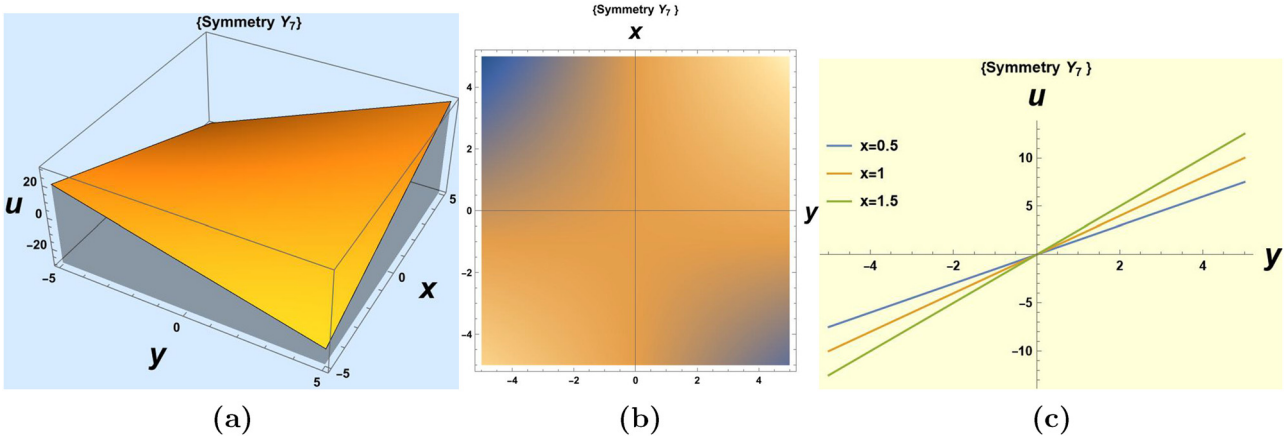

Figure 13: (a) 3D plot showing the solution (2.37) for the parameters $\alpha = k = 1$ and $t = 1, -5 \le y, x \le 5$, (b) 2D density plot, and (c) 2D plot of solution (2.37) depicted on the interval $-5 \le y \le 5$.

$\varepsilon_2 = 0$, $\varepsilon_3 = -3$, $k_1 = 1$, $\alpha = 1$, and $y = 1$, over the spatial interval $-1 \le t, x \le 1$. We illustrate the streaming behaviour of the singular soliton solution (2.9) using 3D, density, and 2D plots in Figure 4, with varying parameter values $a_1 = 1$, $a_2 = 1$, $\alpha = 1$, $b = 1$, $c = 1$, and $y = 1$, over the spatial interval $-5 \le t, x \le 5$. Additionally, the soliton solution (2.15) is depicted through 3D, density, and 2D plots, showcasing a kink-shaped wave profile in Figure 5, with parameter values $\alpha = 1$, $c = 1$, and $\mathfrak{B}_0 = 1$, within the interval $-10 \le t, x \le 10$. The dynamics of the soliton solution (2.24) are depicted in Figure 6 through 3D, density, and 2D plots, using various parameter values $\mathfrak{a}_0 = 1$, $\alpha = 1$, $l = 1$, $c = 1$, $c_0 = 4$, $c_1 = 3$, $y = 1$, over the spatial interval $-10 \le t, x \le 10$. Additionally, Figure 6 illustrates the streaming behaviour of the soliton solution (2.25) in 3D, density, and 2D plots, with the following parameter values $\alpha = 1$, $l = 1$, $\mathfrak{a}0 = 1$, $c = 1$, $c_0 = 4$, $c2 = 1$, and $y = 1$, within the same spatial interval. The kink-shaped soliton solution (2.26) is also represented in Figure 8 through 3D, density, and 2D plots, with parameter values $\mathfrak{a}_0 = 1$, $c = 1$, $n = 1$, $s = 1$, $c_0 = 4$, where $y = 1$, over the range $-10 \le t, x \le 10$. Next, we consider the hyperbolic function solution (2.27), which shares similar characteristics with trigonometric functions. Hyperbolic functions have significant real-world applications, such as in the catenary, the curve formed by a hanging cable or chain under its own weight when supported only at its ends. These functions also appear in various fields, including fluid dynamics, electromagnetic theory, and general relativity, where they describe waveforms and propagation behaviours. Their relevance in our solutions is therefore notable. The dynamical behaviour of the solution (2.27) is presented in Figure 9 through 3D, density, and 2D plots, exhibiting a kink-shaped profile. The parameter values used are $\alpha = 1$, $l = -1$, $\mathfrak{a}_0 = 1$, $c = 1$, $n = 1$, $s = 1$, $c_0 = 4$, where $y = 1$, over the interval $-10 \le t, x \le 10$. It is important to note that, in comparison with other studies cited in the introduction, these results are novel and have not been previously presented in the literature.

4 Conservation laws

To ascertain the conservation laws inherited in the model under consideration, we adopt two distinct methodologies within this section of this study: specifically, the multiplier method [25] and Ibragimov's method [31].

4.1 Conserved vectors through the multiplier method

The multiplier approach is esteemed for its effectiveness in addressing conserved quantities of DEs, irrespective of whether they adhere to variational principles. It is pertinent to note that the zeroth- and first-order multipliers yield no significant results. Consequently, we turn our attention to the second-order multiplier, denoted as $\mathcal{R} = \mathcal{R}(t, x, u, u_t, \ldots, u_{yy})$, and utilize these multipliers to establish the conservation laws governing (1.1). The determination of second-order multipliers, is contingent upon solving the determining equation, leading to the expression

$$\frac{\delta}{\delta u}\{\mathcal{R}(u_t + a u_x u_y + u_{xxy})\} = 0, \tag{4.1}$$

where $\delta/\delta u$ is the Euler operator given by

$$\frac{\delta}{\delta u} = \frac{\partial}{\partial u} - D_t\frac{\partial}{\partial u_t} - D_x\frac{\partial}{\partial u_x} - D_y\frac{\partial}{\partial u_y} + D_{xx}^2 D_y\frac{\partial}{\partial u_{xxy}} + \cdots .$$

By expanding (4.1), we obtain the system of determining equations, which upon simplification and solving gives

$$\mathcal{R} = \mathfrak{C}_1 u_{xx} + \mathfrak{C}_2 u_{yy}, \tag{4.2}$$

where $\mathfrak{C}_1$ and $\mathfrak{C}_2$ are the constants. Now, the conserved quantities can be determined using

$$D_t T^t + D_x T^x + D_y T^y = \mathcal{R}\{u_t + a u_x u_y + u_{xxy}\} \tag{4.3}$$

known as the divergence identity, where T^t denotes the conserved density and T^x and T^y represent the spatial fluxes [25]. Following a sequence of computational procedures, we present herein the conserved vectors associated with the two multipliers.

Case 1. Employing multiplier $\mathcal{R}_1 = u_{xx}$, we derive the associated conserved vector (T_1^t, T_1^x, T_1^y) with its components expressed as

$$\begin{aligned}
T_1^t &= \frac{1}{2}uu_{xx},\\
T_1^x &= \frac{1}{3}au_x{}^2u_y - \frac{1}{3}uau_xu_{xy} - \frac{1}{2}uu_{tx} - \frac{1}{6}uu_{xxxy} + \frac{1}{2}u_tu_x\\
&\quad + \frac{1}{3}u_xu_{xxy} + \frac{1}{3}u_{xx}u_{xy} - \frac{1}{6}u_{xxx}u_y,\\
T_1^y &= \frac{1}{3}auu_xu_{xx} + \frac{1}{6}uu_{xxxx} - \frac{1}{6}u_xu_{xxx} + \frac{1}{6}u_{xx}{}^2.
\end{aligned}$$

Case 2. Utilization of the multiplier $\mathcal{R}_2 = u_{yy}$ yields the associated conserved vector with components

$$\begin{aligned}
T_2^t &= \frac{1}{2}uu_{yy},\\
T_2^x &= \frac{1}{3}auu_yu_{yy} + \frac{1}{3}uu_{xyyy} - \frac{1}{6}u_xu_{yyy} + \frac{1}{3}u_{xy}u_{yy} - \frac{1}{6}u_{xyy}u_y,\\
T_2^y &= \frac{1}{3}au_xu_y{}^2 - \frac{1}{3}uau_yu_{xy} - \frac{1}{2}uu_{ty} - \frac{1}{3}uu_{xxyy} + \frac{1}{2}u_tu_y\\
&\quad - \frac{1}{6}u_xu_{xyy} + \frac{1}{6}u_{xx}u_{yy} + \frac{1}{2}u_{xxy}u_y.
\end{aligned}$$

4.2 Conserved vectors through Ibragimov's theorem

Ibragimov's theorem, a significant advancement in the realm of DEs, extends the renowned Noether's theorem and offers a more comprehensive approach to finding conservation laws for a wider class of DEs. According to this theorem, every infinitesimal, Lie–Bäcklund, or nonlocal symmetry of the system results in a corresponding conservation law [31]. In our study, we leverage Ibragimov's theorem to compute the conserved vectors associated with Eq. (1.1). For a more detailed understanding of this approach, interested readers are encouraged to refer previous study [31].

The adjoint equation for the 2DKdV model (1.1) is

$$\mathcal{M}^* \equiv -2au_{xy}v - v_t - au_xv_y - au_yv_x - v_{xxy} = 0, \quad (4.4)$$

which is obtained from

$$\mathcal{M}^* \equiv \frac{\delta}{\delta u}[v\{u_t + au_xu_y + u_{xxy}\}] = 0,$$

where v depends on t, x, and y. It is noted that since Eq. (4.4) when $u = v$ is not identical to the original model (1.1), we conclude that the 2DKdV model (1.1) is not self-adjoint [31]. The formal Lagrangian for Eq. (1.1) and the adjoint Eq. (4.4) is

$$\mathcal{L} = v\{u_t + au_xu_y + u_{xxy}\}. \quad (4.5)$$

For each infinitesimal symmetry admitted by the 2DKdV model, we derive the conserved vector (T^t, T^x, T^y) by using

$$\begin{aligned} T^i = {} & \xi^i\mathcal{L} + W\left[\frac{\partial\mathcal{L}}{\partial u_i} - D_j\left(\frac{\partial\mathcal{L}}{\partial u_{ij}}\right) + D_jD_k\left(\frac{\partial\mathcal{L}}{\partial u_{ijk}}\right) - \cdots\right] \\ & + D_j(W)\left[\frac{\partial\mathcal{L}}{\partial u_{ij}} - D_k\left(\frac{\partial\mathcal{L}}{\partial u_{ijk}}\right) + \cdots\right] \\ & + D_jD_k(W)\left[\frac{\partial\mathcal{L}}{\partial u_{ijk}} - \cdots\right], \end{aligned}$$

where

$$W = \eta - \xi^j u_j.$$

We have the following eight cases.

Case 1. For $C_1 = \partial/\partial t$, we have the conserved vector with components

$$\begin{aligned} T_1^t &= au_xu_yv + u_{xxy}v, \\ T_1^x &= \frac{1}{3}v_yu_{tx} - au_tu_yv - \frac{2}{3}vu_{txy} - \frac{2}{3}u_tv_{xy} + \frac{1}{3}v_xu_{ty}, \\ T_1^y &= \frac{1}{3}v_xu_{tx} - au_tu_xv - \frac{1}{3}u_{txx}v - \frac{1}{3}u_tv_{xx}. \end{aligned}$$

Case 2. For symmetry $C_2 = \partial/\partial x$, we obtain the conserved vector that has its components given by

$$\begin{aligned} T_2^t &= -u_xv, \\ T_2^x &= \frac{1}{3}u_{xxy}v + u_tv + \frac{1}{3}v_xu_{xy} - \frac{2}{3}u_xv_{xy} + \frac{1}{3}u_{xx}v_y, \\ T_2^y &= \frac{1}{3}u_{xx}v_x - au_x^2v - \frac{1}{3}u_{xxx}v - \frac{1}{3}u_xv_{xx}. \end{aligned}$$

Case 3. Utilizing the symmetry $C_3 = \partial/\partial y$, we obtain the conserved vector

$$\begin{aligned} T_3^t &= -u_yv, \\ T_3^x &= \frac{1}{3}v_yu_{xy} - au_y^2v - \frac{2}{3}u_{xyy}v - \frac{2}{3}u_yv_{xy} + \frac{1}{3}u_{yy}v_x, \\ T_3^y &= \frac{2}{3}u_{xxy}v + u_tv + \frac{1}{3}v_xu_{xy} - \frac{1}{3}u_yv_{xx}. \end{aligned}$$

Case 4. The symmetry $C_4 = \partial/\partial u$ gives conserved vector with components

$$\begin{aligned} T_4^t &= v, \\ T_4^x &= au_yv + \frac{2}{3}v_{xy}, \\ T_4^y &= au_xv + \frac{1}{3}v_{xx}. \end{aligned}$$

Case 5. Employing the symmetry $C_5 = t\partial/\partial t + y\partial\partial y$, we obtain

$$\begin{aligned} T_5^t &= atu_xu_yv - yu_yv + tu_{xxy}v, \\ T_5^x &= \frac{1}{3}tv_xu_{ty} - ayu_y^2v - atu_tu_yv - \frac{2}{3}u_{xy}v - \frac{2}{3}yu_{xyy}v - \frac{2}{3}tvu_{txy} \\ &\quad - \frac{2}{3}tu_tv_{xy} + \frac{1}{3}tv_yu_{tx} + \frac{1}{3}u_yv_x - \frac{2}{3}yu_yv_{xy} + \frac{1}{3}yu_{yy}v_x \\ &\quad + \frac{1}{3}yv_yu_{xy}, \\ T_5^y &= \frac{2}{3}yu_{xxy}v - atu_tu_xv + yu_tv - \frac{1}{3}tu_{txx}v - \frac{1}{3}tu_tv_{xx} + \frac{1}{3}tv_xu_{tx} \\ &\quad + \frac{1}{3}yv_xu_{xy} - \frac{1}{3}yu_yv_{xx}. \end{aligned}$$

Case 6. The symmetry $C_6 = at\partial/\partial t + x\partial/\partial u$ gives the conserved vector with components

$$\begin{aligned} T_6^t &= xv - atu_yv, \\ T_6^x &= axu_yv - axu_yva^2tu_y^2v - \frac{2}{3}atu_{xyy}v - \frac{2}{3}atu_yv_{xy} + \frac{1}{3}atu_{yy}v_x \\ &\quad + \frac{1}{3}atv_yu_{xy} + \frac{2}{3}xv_{xy} - \frac{v_y}{3}, \\ T_6^y &= axu_xv + \frac{2}{3}atu_{xxy}v + atu_tv + \frac{1}{3}atv_xu_{xy} - \frac{1}{3}atu_yv_{xx} - \frac{v_x}{3} \\ &\quad + \frac{1}{3}xv_{xx}. \end{aligned}$$

Case 7. From the infinitesimal symmetry $C_7 = at\partial/\partial t + y\partial/\partial u$, one obtains

$$T_7^t = yv - atu_xv,$$
$$T_7^x = ayu_yv + \frac{1}{3}atu_{xxy}v + atu_tv + \frac{1}{3}atv_xu_{xy} - \frac{2}{3}atu_xv_{xy} + \frac{1}{3}atu_{xx}v_y + \frac{2}{3}yv_{xy} - \frac{v_x}{3},$$
$$T_7^y = ayu_xv - a^2tu_x^2v - \frac{1}{3}atu_{xxx}v - \frac{1}{3}atu_xv_{xx} + \frac{1}{3}atu_{xx}v_x + \frac{1}{3}yv_{xx}.$$

Case 8. Finally for the symmetry $C_8 = x\partial/\partial x - 2y\partial/\partial y - u\partial/\partial u$, we have

$$T_8^t = 2yu_yv - xu_xv - uv,$$
$$T_8^x = 2ayu_y^2v - au_yuv - \frac{2}{3}v_{xy}u + \frac{4}{3}yu_{xyy}v + \frac{1}{3}xu_{xxy}v + xu_tv - \frac{1}{3}u_yv_x + \frac{4}{3}yu_yv_{xy} + \frac{2}{3}u_xv_y - \frac{2}{3}yu_{yy}v_x - \frac{2}{3}yv_yu_{xy} + \frac{1}{3}xv_xu_{xy} - \frac{2}{3}xu_xv_{xy} + \frac{1}{3}xu_{xx}v_y,$$
$$T_8^y = \frac{1}{3}xu_{xx}v_x - axu_x^2v - au_xuv - u_{xx}v - \frac{1}{3}v_{xx}u - \frac{4}{3}yu_{xxy}v - \frac{1}{3}xu_{xxx}v - 2yu_tv - \frac{2}{3}yv_xu_{xy} + \frac{2}{3}yu_yv_{xx} + \frac{2}{3}u_xv_x - \frac{1}{3}xu_xv_{xx}.$$

Remark. The inclusion of the variable v in the conserved vectors derived through Ibragimov's technique suggests that the DE under consideration exhibits an infinite set of conserved vectors. Furthermore, it is noteworthy that the obtained conserved vectors have been rigorously verified across all cases to satisfy the divergence identity. This meticulous validation ensures the robustness and reliability of the derived conserved quantities, affirming their significance in characterizing the underlying dynamics of the system.

5 Discussion of results obtained in this work

As delineated and extensively discussed in the introduction, prior investigations into the novel 2DKdV model have employed diverse methodologies to procure exact solutions. In our study, we harness the potent Lie symmetry method, which, *via* symmetry reductions, facilitates the discovery of fresh exact solutions. Additionally, we employ methodologies such as Kudryashov's method, the simplest equation technique, direct integration, and the power series method, all of which, to the best of our knowledge, have not been previously employed in this context. Similar to earlier researchers, we successfully unearth solutions expressed in trigonometric, hyperbolic, and exponential functions. However, our investigation constitutes a noteworthy advancement as we unveil, for the first time in the literature, solutions articulated in terms of Jacobi elliptic functions, alongside certain rational and power series solutions of the model. Furthermore, we establish conserved vectors for the model. These conserved vectors signify the perpetuation of fundamental physical quantities such as the conservation of energy, momentum, and dilation current. Specifically, we discern that time translation symmetry corresponds to energy conservation, spatial translation symmetries are intertwined with the conservation of momentum, and scaling symmetry engenders the conservation of dilation current. These elucidated conservation laws, elucidated in our research, bear significant implications within the ambit of physical sciences, furnishing deeper insights into the underlying dynamics of the 2DKdV model and its practical applications.

6 Concluding remarks

This investigation delved into a comprehensive analysis of the new 2DKdV equation, which holds paramount importance in the realms of ion acoustic waves in plasma and acoustic waves in harmonic crystals. The research methodology employed a multi-faceted approach, incorporating Lie symmetry analysis of DEs alongside Kudryashov's method, the simplest equation technique, direct integration, and the power series method.

Through the application of these analytical tools, solutions for the equation were successfully derived, encompassing a diverse range of functional forms including rational, exponential, hyperbolic, and elliptic functions. These solutions were rigorously validated, affirming their efficacy in representing solutions for the original equation. To visually portray the outcomes, 2D and 3D plots were generated, showcasing kink-shaped, periodic, and multi-wave profiles. These newly acquired exact solutions pave the way for subsequent exploration through numerical analyses, offering the prospect of attaining deeper insights into the model.

The effectiveness of the symmetry transformation method in obtaining analytical solutions was clearly demonstrated through the obtained results. Furthermore, the investigation extended to ascertain the conserved vectors associated with the equation, by employing the multiplier method and Ibragimov's theorem. The exact solutions

and conservation laws presented in this study are anticipated to find significant applications across diverse fields within mathematical physics, offering valuable insights for interpreting various physical phenomena.

Acknowledgments: The authors express their gratitude to the Mafikeng campus of North-West University for their ongoing assistance.

Funding information: MYT Lephoko would like to thank the Council for Scientific and Industrial Research (CSIR) of South Africa for funding this work.

Author contributions: Methodology: MYTL and CMK; software: MYTL; writing original draft: MYTL; writing-review and editing: CMK; visualization: MYTL and CMK; supervision: CMK. All authors have accepted responsibility for the entire content of this manuscript and approved its submission.

Conflict of interest: The authors state no conflict of interest.

Data availability statement: The datasets generated and/or analysed during the current study are available from the corresponding author on reasonable request.

References

[1] Dero S, Fadhel MA, Lund LA, Shah NA. Multiple solutions of unsteady flow of CNTs nanofluid over permeable shrinking surface with effects of dissipation and slip conditions. Mod Phys Lett B. 2024;38(15):2450120.

[2] Albayrak P, Ozisik M, Secer A, Bayram M, Das SE. Optical solitons of stochastic perturbed Radhakrishnan-Kundu-Lakshmanan model with Kerr law of self-phase-modulation. Mod Phys Lett B. 2024;38(15):2450122.

[3] Yang J, Jin M, Xin X. Nonlocal symmetry and exact solutions of the (2+1)-dimensional Gerdjikov-Ivanov equation. Opt Quantum Electron. 2024;56(4):707.

[4] Kumar S, Mohan B, Kumar A. Generalized fifth-order nonlinear evolution equation for the Sawada-Kotera, Lax, and Caudrey-Dodd-Gibbon equations in plasma physics: Painlevé analysis and multi-soliton solutions. Phys Scr. 2022;97(3):035201.

[5] Shehzad K, Seadawy AR, Wang J, Arshad M. The dynamical study and analysis of diverse bright-dark and breathers wave solutions of nonlinear evolution equations and their applications. Mod Phys Lett B. 2023;38(16):2341013.

[6] Gasmi B, Moussa A, Mati Y, Alhakim L, Baskonus HM. Bifurcation and exact traveling wave solutions to a conformable nonlinear Schrödinger equation using a generalized double auxiliary equation method. Opt Quantum Electron. 2024;56(1):18.

[7] Khalique CM, Lephoko MYT. Conserved vectors and solutions of the two-dimensional potential KP equation. Open Phys. 2023;21(1):20230103.

[8] Su T, Li X, Yu H. Lump solutions for a (2+1)-dimensional generalized KP-type equation. Mod Phys Lett B. 2024;38(15):2450128.

[9] Khan MI, Marwat DNK, Sabi'u J, Inc M. Exact solutions of Shynaray-IIA equation (S-IIAE) using the improved modified Sardar sub-equation method. Opt Quantum Electron. 2024;56(3):459.

[10] Qi J, Zhu Q. Further results about the non-travelling wave exact solutions of nonlinear Burgers equation with variable coefficients. Results Phys. 2023;46:106285.

[11] Kumar S, Mohan B, Kumar R. Newly formed center-controlled rouge wave and lump solutions of a generalized (3+1)-dimensional KdV-BBM equation via symbolic computation approach. Phys Scr. 2023;98(8):085237.

[12] Edeki SO, Fadugba SE, Khalique CM. Valuation of deposit insurance Black-Scholes model using Banach contraction principle. Partial Differ Equ Appl. 2023;8:100571.

[13] Márquez AP, de la Rosa R, Garrido TM, Gandarias ML. Conservation laws and exact solutions for time-delayed Burgers-Fisher equations. Mathematics. 2023;11(17):640.

[14] Ali NH, Mohammed SA, Manafian J. Study on the simplified MCH equation and the combined KdV-mKdV equations with solitary wave solutions. Partial Differ Equ Appl. 2023;9:100599.

[15] Afrin FU. Solitary wave solutions and investigation the effects of different wave velocities of the nonlinear modified Zakharov-Kuznetsov model for the wave propagation in nonlinear media. Partial Differ Equ Appl. 2023;8:100583.

[16] Alam MN, Islam SR. The agreement between novel exact and numerical solutions of nonlinear models. Partial Differ Equ Appl. 2023;8:100584.

[17] Erdoğan F. A second-order numerical method for singularly perturbed Volterra integro-differential equations with delay. Int J Math Comput Eng. 2024;2(1):85–96.

[18] Malfliet W, Hereman W. The tanh method: I exact solutions of nonlinear evolution and wave equations. Phys Scr. 1996;54:563–8.

[19] Gu CH. Soliton theory and its application. Zhejiang: Zhejiang Science and Technology Press; 1990.

[20] Rahman MA. The exp $(-\Phi(\eta))$-expansion method with application in the (1+1)-dimensional classical Boussinesq equations. Results Phys. 2014;4:150–5.

[21] Salas AH, Gomez CA. Application of the Cole–Hopf transformation for finding exact solutions to several forms of the seventh-order KdV equation. Math Probl Eng. 2010;2010(1):194329.

[22] Weiss J, Tabor M, Carnevale G. The Painlévé property and a partial differential equations with an essential singularity. Phys Lett A. 1985;109:205–8.

[23] Kudryashov NA, Loguinova NB. Extended simplest equation method for nonlinear differential equations. Appl Math Comput. 2008;205:396–402.

[24] Ovsiannikov LV. Group analysis of differential equations. New York: Academic Press; 1982.

[25] Olver PJ. Applications of Lie groups to differential equations. second ed., Berlin: Springer-Verlag; 1993.

[26] Naz R, Mahomed FM, Mason DP. Comparison of different approaches to conservation laws for some partial differential equations in fluid mechanics. Appl Math Comput. 2008;205(1: 212–30.

[27] Bluman GW, Kumei S. Symmetries and differential equations. Vol. 81. New York: Springer Science & Business Media; 2013.

[28] Cheviakov AF. Computation of fluxes of conservation laws. J Eng Math. 2010;66:153–73.

[29] Peng L. Symmetries, conservation laws, and Noether's theorem for differential-difference equations. Stud Appl Math. 2017;139(3):457–502.
[30] Noether E. Invariante Variationsprobleme. Gesell Wissen Gottingen Math Phys Kl Heft. 1918;2:235–57.
[31] Ibragimov NH. A new conservation theorem. J Math Anal Appl. 2007;333(1): 311–28.
[32] Arif MG, Islam Z, Begum M, Sheikh MAN. Dynamical behaviors of a new KdV model via Hirota's bilinear formulation. Partial Differ Equ Appl. 2022;6:100410.
[33] Yokus A, Isah MA. Stability analysis and soliton solutions of the nonlinear evolution equation by homoclinic technique based on Hirota bilinear form. International Conference on Fractional Differentiation and Its Applications (ICFDA). IEEE; 2023. p. 1–6.
[34] Isah MA, Yokus A. Rogue waves and stability analysis of the new (2+1)-KdV equation based on symbolic computation method via Hirota bilinear form. International Conference on Fractional Differentiation and Its Applications (ICFDA). IEEE; 2023. p. 1–6.
[35] Raheel M, Zafar A, Liu JG. New periodic-wave, periodic-cross-kink wave, three wave and other analytical wave solitons of new (2+1)-dimensional KdV equation. Eur Phys J Plus. 2024;139(1):50.
[36] Kumar S, Kumar D, Kumar DA. Lie symmetry analysis for obtaining the abundant exact solutions, optimal system and dynamics of solitons for a higher-dimensional Fokas equation. Chaos Solit Fractals. 2021;142:110507.
[37] Kudryashov NA. Analytical theory of nonlinear differential equations Moskow-Igevsk: Institute of Computer Investigations; 2004.
[38] Billingham J, King AC. Wave motion. Cambridge: Cambridge University Press; 2000.
[39] Abramowitz M, Stegun I. Exponential function, Abramowitz M. Handbook of mathematical functions. New York: Dover; 1972.
[40] Kudryashov NA. One method for finding exact solutions of nonlinear differential equations. Commun Nonlinear Sci Numer Simul. 2012;17(6):2248–53.
[41] Kudryashov NA. Exact solitary waves of the Fisher equation. Phys Lett A. 2005;342;99–106.
[42] Zhao YM, He YH, Long Y. The simplest equation method and its application for solving the nonlinear NLSE, KGZ, GDS, DS, and GZ equations. J Appl Math. 2013;2013:960798.
[43] Liu H, Li Q, Zhang Q. Lie symmetry analysis and exact explicit solutions for general Burgers' equation. J Comput Appl Math. 2009;228(1):1–9.